

Isolation of Novel Radical Cations from Hydroquinone Ethers. Conformational Transition of the Methoxy Group upon Electron Transfer

Rajendra Rathore and Jay K. Kochi*

Department of Chemistry, University of Houston, Houston, Texas 77204-5641

Received March 1, 1995*

Hydroquinone ethers as the bis-annulated derivatives **R1–R3** are excellent electron donors by virtue of the facile oxidation to their radical cations **R1^{•+}**, **R2^{•+}**, and **R3^{•+}** that are readily isolable as unusually robust SbCl_6^- and BF_4^- salts persistent in air for prolonged periods. Although the gas-phase vertical ionization potentials of the methyl ethers **R1a** and **R2a** are the same ($IP = 7.83 \pm 0.01$ eV), the oxidation potential of **R1a** in dichloromethane solution is less positive than that of **R2a** ($E_{1/2} = 1.11$ and 1.30 V, respectively). The significantly lower value of $E_{1/2}$ for **R1a** relative to **R2a**, despite minimal changes in structure, is attributed to the conformational change that can occur in the radical cation. Indeed, X-ray crystallographic analysis of **R1a**, **R2a**, and **R1a^{•+}** shows that the increased donor strength of **R1a** is derived from the enhanced (resonance) stabilization of **R1a^{•+}**, in which the methoxy group undergoes a 90° rotation to the favorable coplanar conformation with respect to the aromatic ring. The subtle variation in the molecular structures of **R1** and **R2** accounts for the difference in nonbonded steric effects arising from the bridgehead α -hydrogens toward the methoxy groups.

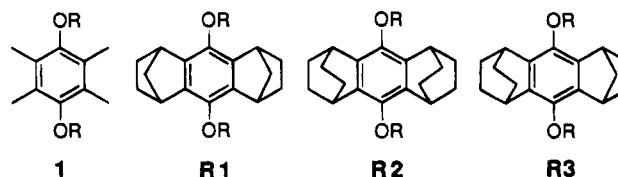
Introduction

Methoxy substituents confer enhanced donor properties upon various aromatic compounds. As such, polymethoxyphenyl moieties are abundant in a variety of natural products such as lignins, vitamin E (tocopherol), psychotomimetic entities, *etc.*^{1–4} that are important in various medicinal uses as antioxidants and as building blocks in mesogenic materials.^{5,6} Particularly pertinent is understanding the role of the conformation of the methoxy groups on the donor properties of substituted methoxyarenes,^{7–9} since substituents *ortho* to the methoxy group can inhibit the resonance interaction between the methoxy group and the π -system of the aromatic ring as a result of nonbonded interactions of the proximate substituents that force the methyl of the methoxy group to lie in the regions perpendicular to either side of the aromatic ring. Consequently, the electron-releasing ef-

fect of the methoxy group can be considerably compromised by a pair of *ortho* substituents.

Recently, we reported¹⁰ on the electrochemical oxidation potentials of a complete series of polymethyl-substituted *p*-hydroquinone ethers in which the values of $E_{1/2}$ followed an unusual trend with the number of methyl substituents. Thus, the tetramethyl derivative **1a** ($R = \text{CH}_3$) was irreversibly oxidized at the most positive potential of $E_{1/2} = 1.48$ V that is similar to that of the unsubstituted parent *p*-dimethoxybenzene ($E_{1/2} = 1.35$ V).¹¹ In contrast, the intermediate dimethyl derivative 2,5-dimethyl-1,4-dimethoxybenzene was the best electron donor ($E_{1/2} = 1.02$ V) of the series. Indeed, the substitution pattern and not the number of methyl groups appeared to be the most important determinant for $E_{1/2}$. In this regard, the donor behavior of the polymethyl-*p*-dialkoxybenzenes was quite distinct from that of the polymethylbenzenes, in which previous studies showed that $E_{1/2}$ decreased monotonically with the number of methyl substituents (independent of the substitution pattern).¹²

In order to gain a better insight into the effect of substituents on the electron donor properties of hydroquinone ethers, we have designed a series of sterically encumbered derivatives **R1–R3** with graded donor strengths (*i.e.* oxidation potentials). We now report that



these annulated tetrasubstituted hydroquinone ethers are unusually effective electron donors, and they form

* Abstract published in *Advance ACS Abstracts*, July 1, 1995.

(1) (a) Ayres, D. C.; Loike, J. D. *Lignans: Chemical, Biological, Chemical Properties*; Cambridge University Press: Cambridge, 1990. (b) Ward, R. S. *Tetrahedron* **1990**, *46*, 5029. (c) Ward, R. S. *Nat. Prod. Rep.* **1993**, *10*, 1.

(2) (a) Machlin, L. J., Ed. *Vitamin E: A Comprehensive Treatise*; Dekker: New York, 1980; Vol. 1. (b) Burton, G. W.; Ingold, K. U. *J. Am. Chem. Soc.* **1981**, *103*, 6472. (c) Mukai, K.; Daifuku, K.; Okabe, K.; Tanigaki, T.; Inoue, K. *J. Org. Chem.* **1991**, *56*, 4188.

(3) Draper, H. H. In *Atmospheric Oxidation and Antioxidants*; Scott, G., Ed.; Elsevier: New York, 1993; Vol. 3.

(4) (a) Sener, B.; Temizer, H.; Konukol, S.; Koyuncu, M. In *Advances in Natural Product Chemistry*; Rahman, A., Ed.; Harwood: New York, 1992. (b) Connolly, J. D. In *Natural Products Chemistry 1984*; Zalewski, R. I.; Skolik, J. J., Eds.; Elsevier: New York, 1985. (c) Semmelhack, M. F.; Helquist, P.; Jones, L. D.; Keller, L.; Mendelson, L.; Ryono, L. S.; Smith, J. G.; Stauffer, R. D. *J. Am. Chem. Soc.* **1981**, *103*, 6460.

(5) Suarna, C.; Baca, M.; Sothwell-Keely, T. *Lipids* **1992**, *42*, 447 and references cited therein.

(6) (a) Counsell, C. J. R.; Emsley, J. W.; Luckhurst, G. R.; Sachdev, H. S. *Mol. Phys.* **1988**, *63*, 33. (b) Goodby, J. W.; Hird, M.; Toyne, K. J.; Watson, T. *J. Chem. Soc., Chem. Commun.* **1994**, 1701.

(7) (a) Schaefer, T.; Sebastian, R. *Can. J. Chem.* **1989**, *67*, 1148. (b) See also Burton and Ingold in ref 2b.

(8) Jardon, P. W.; Vickery, E. H.; Pahler, L. F.; Pourahmady, N.; Mains, G. J.; Eisenbraun, E. J. *J. Org. Chem.* **1984**, *49*, 2130.

(9) Pandiarajan, K.; Kabilan, S.; Sankar, P.; Kolehmainen, E.; Nevalainen, T.; Kauppinen, R. *Bull. Chem. Soc. Jpn.* **1944**, *67*, 2639 and references cited therein.

(10) Rathore, R.; Bosch, E.; Kochi, J. K. *Tetrahedron* **1994**, *50*, 6727.

(11) Furthermore, dimethoxydurene (**1a**) is the only member in this series to show irreversible CV behavior at $\nu = 0.1$ V s⁻¹.

(12) Howell, J. O.; Goncalves, J. M.; Amatore, C.; Klasinc, L.; Wightman, R. M.; Kochi, J. K. *J. Am. Chem. Soc.* **1984**, *106*, 3968.

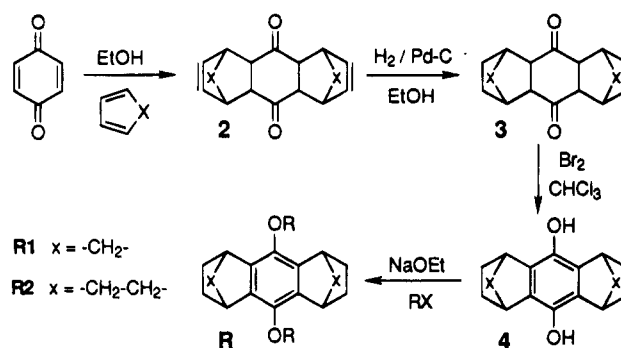
exceptionally stable aromatic radical cation salts upon chemical or electrochemical oxidation. The highly colored paramagnetic salts can be isolated and stored as crystalline solids for an indefinite period. The latter is noteworthy since radical cations can be important intermediates in a rich menu of organic transformations, and they are useful as electron transfer catalysts.^{13,14} Most noteworthy is the conformational changes that can occur upon the redox transformation of the neutral donors **R1a–R3a** (methoxy groups perpendicular to the aromatic plane) to the radical cation (methoxy groups in the aromatic plane) that is established with the aid of NMR spectroscopy, X-ray crystallography, electrochemistry, and photoelectron spectroscopy. To date, the only radical cations readily accessible to organic chemists are the heteroatom-centered tris(4-bromophenyl)aminium¹⁵ and thianthrenium salts,¹⁶ which have been extensively used in the elucidation of the reaction mechanisms and in organic synthesis.^{17,18}

Results

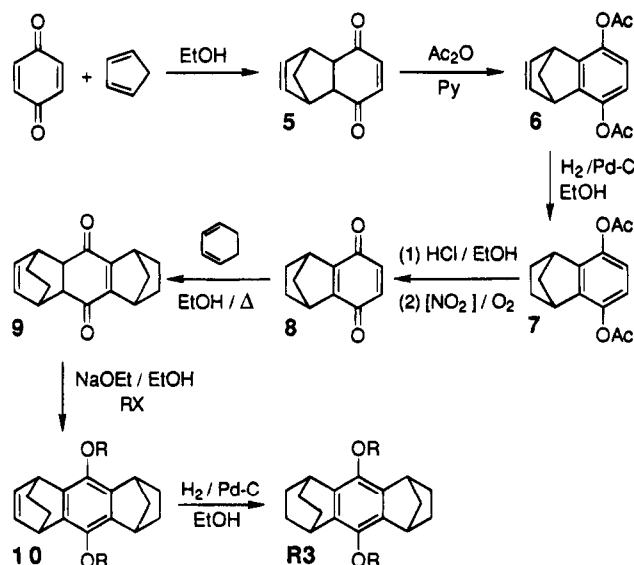
Synthesis of Annulated Hydroquinone Ethers as Electron Donors. The symmetrically bridged *p*-dialkoxybenzenes (**R1** and **R2**) were readily prepared from the corresponding hydroquinones, which were obtained from the Diels–Alder condensation¹⁹ of *p*-benzoquinone with cyclopentadiene and cyclohexadiene, respectively, according to Scheme 1. Low-pressure hydrogenation of Diels–Alder adducts **2** over a palladium/carbon catalyst afforded the saturated diketones **3** in quantitative yield. Aromatization of the diketones **3** to the corresponding hydroquinones **4** was accomplished with an equimolar amount of bromine in anhydrous chloroform. The hydroquinones were then alkylated with various alkyl halides (RX) and potassium hydroxide in ethanol to afford the hydroquinone ethers **R1** and **R2** in excellent overall yields.

The unsymmetrically bridged *p*-dialkoxybenzenes (**R3**) were prepared by stepwise condensation of two different dienes with *p*-benzoquinone as illustrated in Scheme 2.

Scheme 1



Scheme 2



Thus, the reaction of *p*-benzoquinone with cyclopentadiene in ethanol afforded the monoadduct **5** which was directly converted to the aromatized diacetate **6** using acetic anhydride and pyridine in 94% isolated yield according to Meinwald *et al.*²⁰ The unsaturated diacetate **6** upon catalytic hydrogenation over palladium/carbon afforded the saturated analogue **7** quantitatively. The diester **7** was transformed to the quinone **8** in quantitative yield by acid-catalyzed hydrolysis of the diester **7** to the corresponding hydroquinone, followed by a facile autooxidation using a catalytic amount of nitrogen dioxide.²¹ The reaction of quinone **8** with cyclohexadiene afforded the adduct **9**, which was directly converted to the corresponding dialkoxybenzenes **10** (see the Experimental Section). Catalytic hydrogenation of **10** afforded the *p*-dialkoxybenzenes **R3** in excellent yields.

Structural Characterization of the Hydroquinone Ethers. X-Ray Crystallographic Structure Analysis. In order to ascertain the conformation of alkoxy groups in the annulated hydroquinone ethers, we obtained the crystal structures of **R1a** and **R2a**³⁸ (R = CH₃). Thus, colorless needle-like crystals of **R1a** suitable for X-ray crystallographic analysis were grown by the slow evaporation of a hexane solution of the ether. The crystals belonged to the monoclinic space group *P2*₁/*C*. The intensity data were collected on a Nicolet R3m/V automatic diffractometer, and the structure determina-

(13) (a) Pandey, G. *Top. Curr. Chem.* **1993**, *168*, 175. (b) Kochi, J. K. In *Comprehensive Organic Synthesis*; Trost, B. M., Ed.; Pergamon: New York, 1991; Vol. 7, p 849. (c) Kochi, J. K. *Adv. Free Radical Chem. (Greenwich, Conn.)* **1990**, *1*, 53. (d) Kita, Y.; Tohma, H.; Hatanaka, K.; Takada, T.; Fujita, S.; Mitoh, S.; Sakurai, H.; Oka, S. *J. Am. Chem. Soc.* **1994**, *116*, 3684 and references cited therein. (e) Stewart, R. F.; Miller, L. L. *J. Am. Chem. Soc.* **1980**, *102*, 4999. (f) Cossy, J. *Bull. Soc. Chim. Fr.* **1994**, *131*, 344 and references cited therein. (g) Workentin, M. S.; Johnston, L. J.; Wayner, D. D. M.; Parker, V. D. *J. Am. Chem. Soc.* **1994**, *116*, 8279 and references cited therein.

(14) (a) Chanon, M. *Bull. Soc. Chim. Fr.* **1985**, 209. (b) Bauld, N. L.; Bellville, D. J.; Harirchian, B.; Lorenz, K. T.; Pabon, P. A., Jr.; Reynolds, D. W.; Wirth, D. D.; Chiou, H. S.; Marsh, B. K. *Acc. Chem. Res.* **1987**, *20*, 371. (c) Ebersson, L. *Electron Transfer Reactions in Organic Chemistry*; Springer: New York, 1987.

(15) Bell, F. A.; Ledwith, A.; Sherrington, D. C. *J. Chem. Soc. C* **1969**, 2719.

(16) (a) Lucken, E. A. C. *J. Chem. Soc.* **1969**, 4963. (b) Bandlish, B. K.; Shine, H. J. *J. Org. Chem.* **1977**, *42*, 561 and references cited therein.

(17) (a) Kim, T.; Mirafzal, G. A.; Liu, J.; Bauld, N. L. *J. Am. Chem. Soc.* **1993**, *115*, 7653. (b) Dhanalekshmi, S.; Venkatachalam, C. S.; Balasubramanian, K. K. *J. Chem. Soc., Chem. Commun.* **1994**, 511 and references cited therein. (c) Shine, H. J.; Yueh, W. *Tetrahedron Lett.* **1992**, *33*, 6583. (d) Hammerich, O.; Parker, V. D. *Acta Chem. Scand.* **1982**, *B36*, 421 and references cited therein. (e) Nelsen, S. F.; Akaba, R. *J. Am. Chem. Soc.* **1981**, *103*, 2096. (f) Hammerich, O.; Parker, V. D. *Adv. Phys. Org. Chem.* **1984**, *20*, 55.

(18) (a) Bauld, N. L. *Tetrahedron* **1989**, *45*, 5307 and references cited therein. (b) Schmittel, M. *Top. Curr. Chem.* **1994**, *169*, 183 and references cited therein. (c) Mirafzal, G. A.; Liu, J.; Bauld, N. L. *J. Am. Chem. Soc.* **1993**, *115*, 6072. (d) Engel, P. S.; Robertson, D. M.; Scholz, J. N.; Shine, H. J. *J. Org. Chem.* **1992**, *57*, 6178.

(19) Alder, K.; Stein, G. *Ann. Chim. (Paris)* **1935**, *501*, 247.

(20) Meinwald, J.; Wiley, G. A. *J. Am. Chem. Soc.* **1958**, *80*, 3667.

(21) (a) Rathore, R.; Bosch, E.; Kochi, J. K. *Tetrahedron Lett.* **1994**, *35*, 1335. (b) Bosch, E.; Rathore, R.; Kochi, J. K. *J. Org. Chem.* **1994**, *59*, 2529.

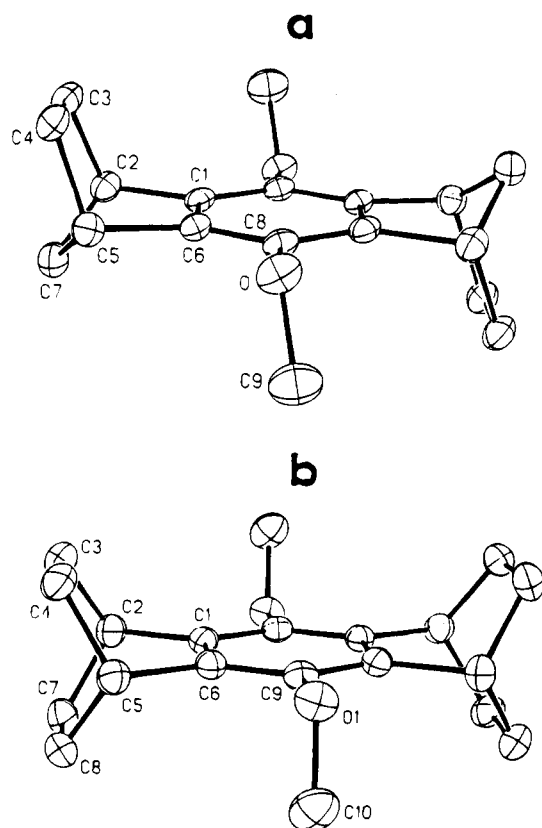


Figure 1. ORTEP diagrams of the annulated hydroquinone ethers (a) **R1a** and (b) **R2a** showing the conformations of the methoxy groups to be perpendicular to the aromatic plane. The hydrogens are omitted for clarity.

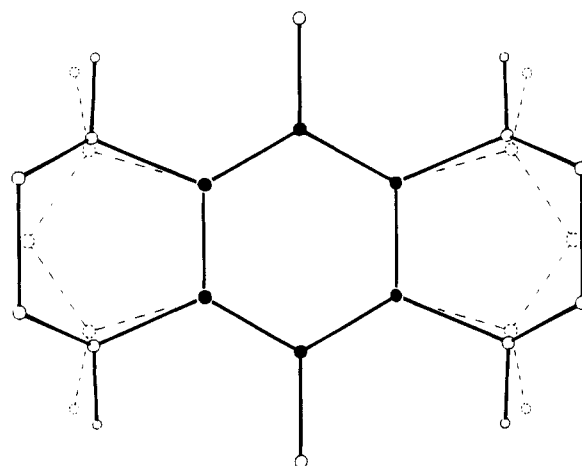
Table 1. Selected Bond Distances (Å) and Angles (deg) for R1a and R2a

R1a		R2a ^a	
Distances			
C1-C6	1.398(3)	C1-C6	1.396(3) 1.402(3)
C6-C8	1.389(2)	C6-C9	1.384(3) 1.389(3)
C8-O	1.391(2)	C9-O	1.388(3) 1.394(3)
C9-O	1.414(3)	C10-O	1.427(3) 1.420(3)
C1-C2	1.516(3)	C1-C2	1.510(3) 1.512(3)
C5-C6	1.518(2)	C5-C6	1.511(2) 1.512(2)
Angles			
C6-C5-C7	99.8(2)	C6-C5-C7	107.7(1) 108.2(2)
C6-C5-C4	106.1(2)	C6-C5-C4	108.8(1) 107.6(1)
C7-C5-C4	100.5(2)	C7-C5-C4	108.8(2) 108.2(2)
C1-C2-C3	106.6(1)	C1-C2-C3	107.6(1) 107.8(1)
C1-C2-C7	100.0(1)	C1-C2-C7	108.1(2) 108.5(1)
C3-C2-C7	100.0(2)	C3-C2-C7	107.9(2) 107.2(2)
C8-O-C9	113.9(1)	C9-O-C10	112.4(2) 114.5(1)

^a The unit cell contains two molecules (*i.e.* $Z = 2$) with the molecular center of symmetry coinciding with the crystallographic inversion center.

tion was carried out using the direct methods program SHELXTL. The crystals of the homologous derivative **R2a** (grown in a similar way) were in the triclinic space group $P\bar{1}$, and the structure determination was accomplished in an analogous manner. The perspective ORTEP views of the molecular structures of **R1a** and **R2a** are shown in Figures 1a and 1b, respectively. The selected bond lengths and angles of interest are recorded in Table 1, which shows that the bond lengths are normal. The methyls of the methoxy groups in both structures were found to be out of the aromatic plane, being almost perpendicular (the torsion angles C6-C8-O-C9 in **R1a** and C6-C9-O-C10 in **R2a** are 99.1 and

Chart 1



101.1°, respectively) as has also been shown in several *ortho*-substituted methoxybenzenes by X-ray crystallography.²² However, significant differences in the bond angles with respect to the bridgehead atoms C2 and C5 were observed. Of particular note is the fact that the hydrogens H2 and H5 attached to C2 and C5, respectively, lie in the plane of the aromatic ring in **R2a**, whereas they are pushed away from the plane (*i.e.* toward the methano carbon) in the case of **R1a** as a consequence of the angular and torsional strain imposed by the bridging of the methano carbon. The resultant increase in the separation of the bridgehead hydrogen from the ethereal (oxygen) center in **R1a** relative to that in **R2a** is illustrated schematically in Chart 1 (note that the view is normal to the aromatic ring taken after the benzenoid carbons of **R1a** (see the filled circles in Chart 1) were arbitrarily superimposed onto the corresponding carbons of **R2a**).

¹H NMR Spectroscopy. Variable-temperature ¹H NMR spectroscopy²³ was used to delineate the conformational mobility of the alkoxy groups in the tetrasubstituted hydroquinone ethyl ethers **R1b** and **R3b** in solution. Thus, the ¹H NMR spectra of ethyl ether derivatives **R1b** and **R3b** ($R = \text{CH}_3\text{CH}_2$) in CDCl_3 or $\text{DMSO-}d_6$ at room temperature showed well-resolved multiplets (see Figure 2) which were attributed to the AB portion of an ABM_3 system for the ethoxy methylenes. The observed chemical shift nonequivalence of the geminal methylene protons of the ethoxy groups at ambient temperature indicated a molecular "dissymmetry" on the NMR time scale. Interestingly, the ABM_3 pattern in **R1b** or **R3b** was unperturbed upon warming (140 °C) or cooling (-60 °C) the sample in the NMR probe. In contrast, the symmetrically substituted **R2b** or the tetramethyl derivative **1b** (in which both faces of the benzene ring are substituted with identical groups, *e.g.* see Figure 1b) showed the normal methylene quartet of an A_2M_3 system at ambient temperature for the ethoxy groups (see Figure 2). Notably, this pattern was also unchanged upon warming (140 °C) or cooling (-90 °C) the NMR probe.

Electrochemical Oxidation of Hydroquinone Ethers. Various annulated *p*-dimethoxybenzenes in series **R1-R3** (Table 2) were oxidized electrochemically

(22) Schuster, I. I.; Parvez, M.; Freyer, A. J. *J. Org. Chem.* **1988**, *53*, 5819.

(23) Oki, M. *Applications of Dynamic NMR Spectroscopy to Organic Chemistry*; VCH: New York, 1985.

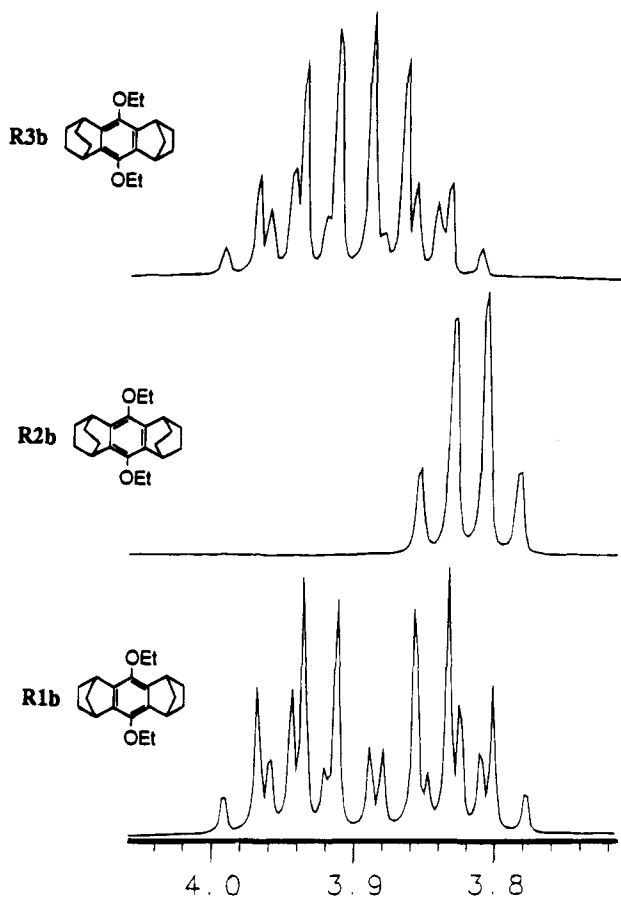
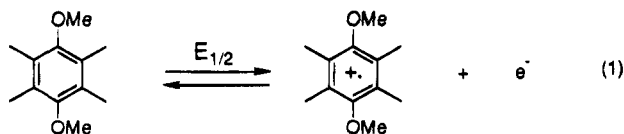


Figure 2. Comparative ^1H NMR (300 MHz) splitting patterns of the methylene protons of the ethoxy groups of the hydroquinone ethers **R1b**, **R2b**, and **R3b** in $\text{DMSO}-d_6$ at room temperature.

at a platinum electrode as 5×10^{-3} M solutions in anhydrous dichloromethane containing 0.2 M tetra-*n*-butylammonium hexafluorophosphate (TBAH) as the supporting electrolyte. Reversible cyclic voltammograms (CV) of the dialkyl ethers **R1**, **R2**, and **R3** were consistently attained at scan rates of $\nu = 25\text{--}400$ mV s^{-1} (see Figure 3a), and they all showed anodic/cathodic peak current ratios of $i_a/i_c = 1.0$ (theoretical) at 25 $^\circ\text{C}$. The calibration of the CV peaks with ferrocene provided the reversible oxidation potentials ($E_{1/2}$) for the production of the cation radicals *via* the one-electron redox couple, *i.e.*



For the sake of comparison, the acyclic tetrasubstituted analogues (**1a** and **1b**) under identical electrochemical conditions showed irreversible anodic peaks (see Table 2) at scan rates up to 5 V s^{-1} . The values of $E_{1/2}$ for the cyclic and acyclic analogues in Table 2 (column 2) followed an unusual trend. For example, the acyclic tetramethyl derivatives (**1**) were oxidized at the most positive potential ($E_{1/2} = 1.48$ V vs SCE), whereas the tetrasubstituted cyclic analogue **R1a** was the best electron donor, as judged by its (most negative) value of the $E_{1/2} = 1.11$ V vs SCE . On the other hand, comparison amongst the three cyclic analogues (**R1**–**R3**) showed

Table 2. Electrochemical Oxidation Potentials of Various Hydroquinone Ethers^a

Hydroquinone Ethers	$E_{1/2}$ (V vs. SCE)	E_p^b (V vs. SCE)
1		
1a R = Me	c	1.56
1b R = Et	c	1.55
R1		
R1a R = Me	1.11	1.15
R1b R = Et	1.11	1.15
R1c R = <i>iso</i> -Propyl	1.10	1.15
R1d R = <i>n</i> -Octyl	1.09	1.14
R1e R = $\text{CH}_2\text{CH}_2\text{OMe}$	1.17	1.21
R2		
R2a R = Me	1.30	1.34
R2b R = Et	1.30	1.34
R2c R = $\text{CH}_2\text{CH}_2\text{OMe}$	1.30	1.34
R3		
R3a R = Me	1.15	1.19
R3b R = Et	1.15	1.19
R3e R = $\text{CH}_2\text{CH}_2\text{OMe}$	1.18	1.22

^a In anhydrous dichloromethane containing 0.2 M $n\text{-Bu}_4\text{N}^+\text{PF}_6^-$ at $\nu = 100$ mV s^{-1} and 25 $^\circ\text{C}$. ^b Anodic (CV) peak potential. ^c Irreversible cyclic voltammogram at $\nu = 100$ mV s^{-1} .

substantial differences in the oxidation potentials (see Figure 3b), despite minimal structural changes on proceeding from **R1** to **R3**. Interestingly, the mixed analogue **R3a** had an intermediate oxidation potential ($E_{1/2} = 1.16$ V) which was closer to that of **R1a** ($E_{1/2} = 1.11$ V) than that of **R2a** ($E_{1/2} = 1.30$ V). The variation of the alkoxy substituents (methyl, ethyl, isopropyl, *n*-octyl) in the hydroquinone ether **R1** led to only slight changes in the oxidation potentials (see Table 2), in accord with the electron-releasing effect of the alkyl groups. However, the substitution of methyl by the 2-methoxyethyl ($\text{CH}_2\text{CH}_2\text{OMe}$) group in hydroquinone ethers **R1a** and **R3a** caused an increase in the oxidation potentials by 60 and 30 mV, respectively. Contrastingly, the corresponding ether **R2e** did not undergo any change in the oxidation potential relative to the methyl ether analogue **R2a** (see Table 2).

Correlation of the Vertical Ionization Potential in the Gas Phase and the Adiabatic Oxidation Potential in Solution. A precise evaluation of the energetics of electron detachment from the various hydroquinone ethers was established from the experimental ionization potentials (IP) as determined from the gas-phase helium(I) photoelectron spectra (PES) at ~ 100 $^\circ\text{C}$.

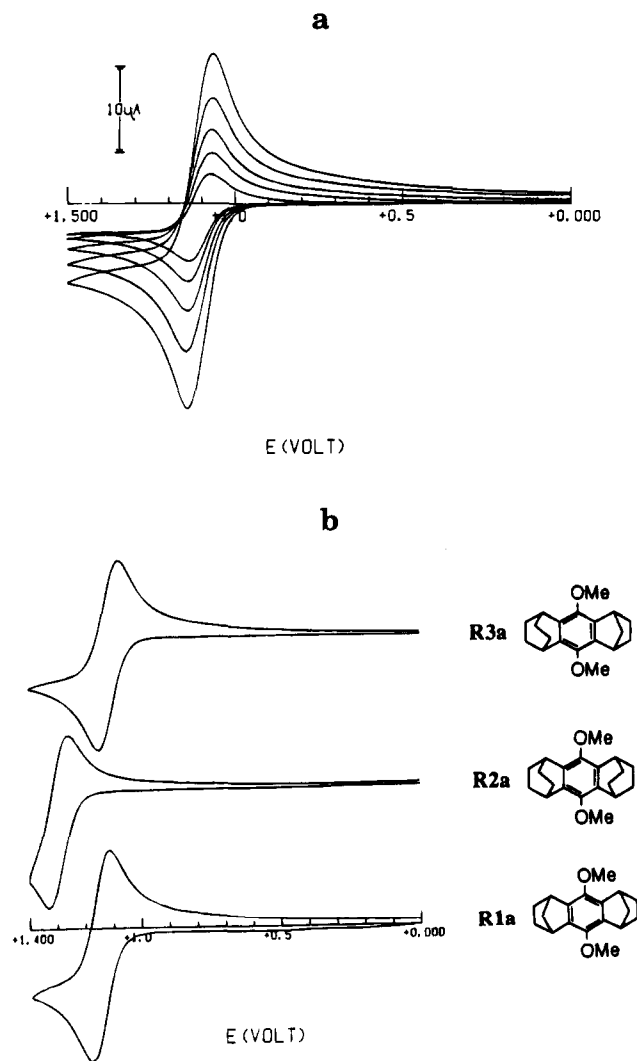


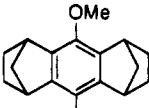
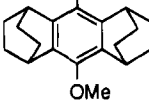
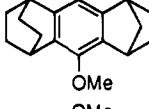
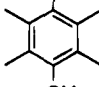
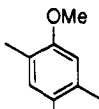
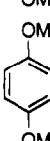
Figure 3. (a) Cyclic voltammogram of 5×10^{-3} M **R1a** in CH_2Cl_2 containing 0.2 M TBAP at sweep rates between $\nu = 25$ – 400 mV s^{-1} . (b) Cyclic voltammograms of 5×10^{-3} M hydroquinone ethers **R1a**, **R2a**, and **R3a** in dichloromethane containing 0.2 M TBAP at a scan rate of 100 mV s^{-1} .

As listed in Table 3, the values of IP's for **R1a**, **R2a**, and **R3a** are almost identical, despite the fact that their reversible oxidation potentials vary by approximately 200 mV. The values of ionization potentials for 1,4-dimethoxybenzene and 2,5-dimethyl-1,4-dimethoxybenzene in Table 3 were taken from the literature.^{24,25} The relationship between the vertical ionization potentials (IP) and the reversible oxidation potentials ($E_{1/2}$) of the hydroquinone dimethyl ethers listed in Table 3 is illustrated in Figure 4.

Isolation of Crystalline Radical-Cation Salts of Hydroquinone Ethers. In harmony with their reversible oxidation potentials, hydroquinone ethers yielded crystalline radical-cation salts upon oxidation with either antimony pentachloride (SbCl_5) or nitrosonium tetrafluoroborate (NO-BF_4^-) as follows.

Hexachloroantimonate Salts. A colorless solution of hydroquinone ether **R1a** in dichloromethane was cooled in a dry ice-acetone bath under an argon atmosphere. When a solution of SbCl_5 in dichloromethane was

Table 3. Comparison of Ionization Potentials (IP) and Reversible Oxidation Potentials ($E_{1/2}$ in V vs SCE) of Various Hydroquinone Ethers

Hydroquinone Ethers	$E_{1/2}^a$ (V vs. SCE)	IP ^b (eV)
R1a 	1.11	7.84
R2a 	1.30	7.83
R3a 	1.15	7.85
1a 	e	8.06
2a 	1.02	7.45 ^c
3a 	1.35	7.90 ^d

^a In dichloromethane solution containing 0.2 M $n\text{-Bu}_4\text{N}^+\text{PF}_6^-$ at $\nu = 100$ mV s^{-1} and 25 $^\circ\text{C}$. ^b At 100 $^\circ\text{C}$, unless indicated otherwise. ^c At ambient temperature from ref 25. ^d At ambient temperature from ref 24. ^e Irreversible cyclic voltammogram at $\nu = 100$ mV s^{-1} .

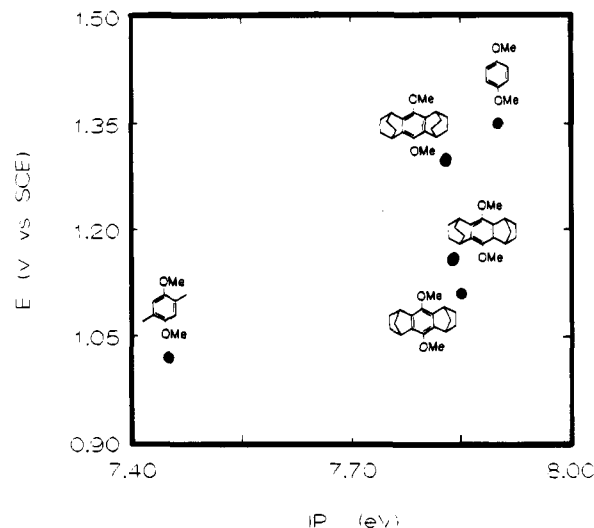


Figure 4. Correlation of the vertical ionization potentials (IP) of various hydroquinone ethers in the gas phase with the adiabatic oxidation potentials ($E_{1/2}$) in dichloromethane solution.

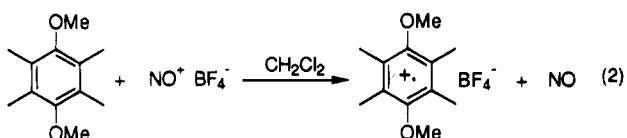
added slowly at -78 $^\circ\text{C}$, the colorless solution instantaneously turned deep red and the deep red-orange crystals of 9,10-dimethoxy-1,4:5,8-dimethanoanthracene hexachloroantimonate salt were obtained in es-

(24) Bock, H.; Wagner, G. *Tetrahedron Lett.* **1971**, 3713.

(25) Gleiter, R.; Schäfer, W.; Staab, H. A. *Chem. Ber.* **1988**, *121*, 1257.

entially quantitative yield (98%). The radical cation salt $\mathbf{R1a}^{\cdot+}\text{SbCl}_6^-$ stored in air persisted indefinitely at room temperature (note that no perceptible color change was observed when the solutions of $\mathbf{R1a}^{\cdot+}$ in dry dichloromethane were exposed to ordinary roomlight for a period of several days at room temperature). The other hydroquinone ethers $\mathbf{R1}$, $\mathbf{R2}$, and $\mathbf{R3}$ in Table 2 were similarly converted to the corresponding radical cation salts in excellent yields and stored under an argon atmosphere.

Tetrafluoroborate Salts. A solution of $\mathbf{R1a}$ in anhydrous dichloromethane was added to crystalline nitrosonium tetrafluoroborate salt under an argon atmosphere at room temperature. Upon continued stirring, the mixture turned dark orange-red. Argon gas was bubbled through the final red solution to entrain the nitric oxide produced in the reaction according to eq 2.²⁷ The mixture was stirred for 0.5 h and cooled to -78°C .

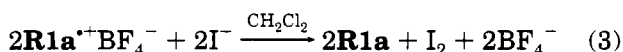


The addition of anhydrous diethyl ether to the red solution led to an orange-red precipitate which was filtered under an argon atmosphere and washed thoroughly with ether and dried *in vacuo* to afford the tetrafluoroborate salt of the radical cation ($\mathbf{R1a}^{\cdot+}$) in excellent yield (note that $\mathbf{R1a}^{\cdot+}\text{BF}_4^-$ salt prepared with NO^+BF_4^- was spectroscopically identical (UV-vis) to the SbCl_6^- salt obtained above). The tetrafluoroborate salts of the radical cations from hydroquinone ethers $\mathbf{R2a}$ and $\mathbf{R3a}$ were also prepared in a similar manner.

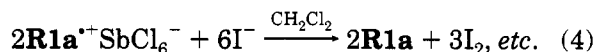
Hexafluorophosphate Salts. Solutions of the radical cations as hexafluorophosphate salts were prepared *in situ* by electrooxidation at the CV anodic peak potentials of $\mathbf{R1a}$, $\mathbf{R2a}$, and $\mathbf{R3a}$ (e.g. for $\mathbf{R1a}$, the oxidation was carried out at 1.12 V) in dichloromethane solutions containing 0.1 M tetrabutylammonium hexafluorophosphate as the supporting electrolyte. The brightly colored solutions of the radical cation salts thus obtained were stable for prolonged periods when protected from moisture.

Determination of the Purity of the Radical-Cation Salts. The purity of the various tetrafluoroborate and hexachloroantimonate salts of the radical cations was determined iodometrically, as follows.

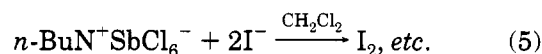
Tetrafluoroborate Salts. The salt $\mathbf{R1a}^{\cdot+}\text{BF}_4^-$ dissolved in dichloromethane reacted rapidly with excess tetra-*n*-butylammonium iodide (TABI) under an argon atmosphere to liberate iodine, which was determined quantitatively by standard thiosulfate titration. Since the re-reduced dimethoxybenzene $\mathbf{R1a}$ was recovered quantitatively, the oxidation of iodide by $\mathbf{R1a}^{\cdot+}\text{BF}_4^-$ can be summarized as



Hexachloroantimonate Salts. The exposure of $\mathbf{R1a}^{\cdot+}\text{SbCl}_6^-$ dissolved in dichloromethane to a solution containing excess TBAI in dichloromethane resulted in the liberation of iodine, the amount of which corresponded to the (partial) stoichiometry in eq 4 (note that the reduced antimony product was not identified). In a



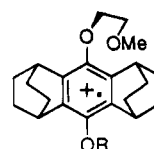
separate control experiment, a solution of tetra-*n*-butylammonium hexachloroantimonate in dichloromethane also reacted with excess TBAI to liberate iodine according to the (partial) stoichiometry in eq 5. Thus, the hexachlo-



roantimonate anion was responsible for the production of excess iodine in the iodometric titrations of the SbCl_6^- salts of the radical cations. The various BF_4^- and SbCl_6^- salts of radical cations $\mathbf{R2a}^{\cdot+}$ and $\mathbf{R3a}^{\cdot+}$ were similarly treated with excess TBAI, and the titration with aqueous thiosulfate indicated the purity of the crystalline salts to be uniformly greater than 98%.

Spectral Properties of the Radical Cations of Hydroquinone Ethers. The electronic absorption spectra of the radical cations derived from hydroquinone ethers showed characteristic twin peaks with one band generally appearing as a partially resolved shoulder.²⁸ For example, the red crystalline $\mathbf{R1a}^{\cdot+}\text{SbCl}_6^-$ salt dissolved in anhydrous dichloromethane displayed the characteristic spectrum shown in the inset of Figure 5a (λ_{max} (nm) = 518, 486 sh). The solutions of $\mathbf{R1a}^{\cdot+}$ followed a simple Beer's Law dependence with an extinction coefficient of $7300 \text{ M}^{-1} \text{ cm}^{-1}$ in dichloromethane at λ_{max} (nm) = 518. The absorption maximum of the $\mathbf{R1a}^{\cdot+}$ obtained from the diffuse reflectance of the crystalline sample was the same as that measured in solution (see Figure 5a). The absorption spectra of the radical-cation salts ($\mathbf{R1}$ – $\mathbf{R3}$) with different counterions (e.g. SbCl_6^- , BF_4^- , PF_6^- , etc.) were rather invariant. A blue (hypsochromic) shift in the absorption spectra was observed on proceeding from $\mathbf{R1a}^{\cdot+}$ (λ_{max} (nm) = 518, 486 sh; $\epsilon = 7300 \text{ M}^{-1} \text{ cm}^{-1}$) to $\mathbf{R3a}^{\cdot+}$ (λ_{max} (nm) = 508, 478 sh; $\epsilon = 6000 \text{ M}^{-1} \text{ cm}^{-1}$) to $\mathbf{R2a}^{\cdot+}$ (λ_{max} (nm) = 486, 464 sh; $\epsilon = 4600 \text{ M}^{-1} \text{ cm}^{-1}$). Such a trend was directly correlated to the reduction potentials of the radical cations (see Figure 5b). The different alkoxy substituents in the radical cations derived from hydroquinone ethers $\mathbf{R1a}$ – \mathbf{e} , $\mathbf{R2a}$ – \mathbf{b} , and $\mathbf{R3a}$ – \mathbf{e} showed no noticeable shifts in the characteristic absorption spectra (see Figure 5b). Interestingly, the radical cation of $\mathbf{R2e}$ (2-methoxyethyl ether derivative) showed a significant difference in its absorption spectrum (with $\lambda_{\text{max}} = 494 \text{ nm}$ shown in Figure 5c) in comparison with that of the methyl ether analogue $\mathbf{R2a}$ ($\lambda_{\text{max}} = 486, 464 \text{ sh}$). The spectral alteration observed in $\mathbf{R2e}^{\cdot+}$, but not in either $\mathbf{R1e}^{\cdot+}$ or $\mathbf{R3e}^{\cdot+}$, is tentatively attributed to the intramolecular participation of the methoxy group (in the out-of-plane sidechain) to the cationic aromatic center.²⁹

Chart 2



(26) Compare: Miller, L. L.; Nordblom, G. D.; Mayeda, E. A. *J. Org. Chem.* **1972**, *37*, 916.

(27) See: Rathore, R.; Bosch, E.; Kochi, J. K. *J. Chem. Soc., Perkin Trans. 2* **1994**, 1157.

(28) Shida, T. *Electronic Absorption Spectra of Radical Ions*; Elsevier: New York, 1988; p 256.

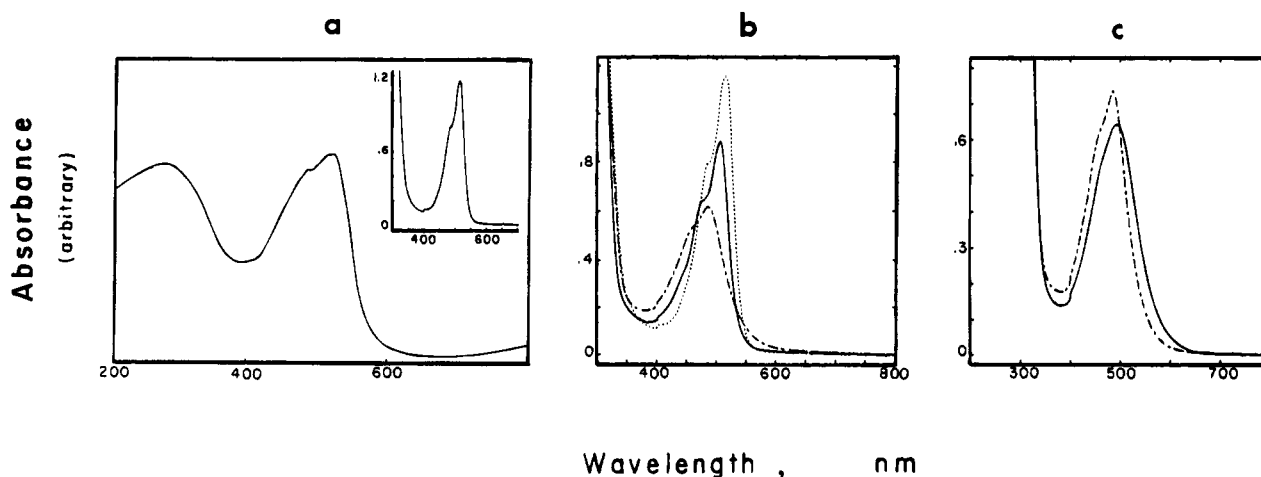


Figure 5. (a) Diffuse reflectance spectrum of crystalline $\mathbf{R1a}^{+\bullet}\text{SbCl}_6^-$ diluted (2%) in alumina. The inset presents the absorption spectrum of $\mathbf{R1a}^{+\bullet}\text{SbCl}_6^-$ in dichloromethane solution. (b) Absorption spectra of 1.6×10^{-4} M hexachloroantimonate salts of $\mathbf{R1a}^{+\bullet}$ (\cdots), $\mathbf{R2a}^{+\bullet}$ ($-\cdots-$), and $\mathbf{R3a}^{+\bullet}$ ($-$) in CH_2Cl_2 at 25 °C. (c) Comparison of the UV-vis absorption spectra of $\mathbf{R2a}^{+\bullet}$ ($-\cdots-$) and $\mathbf{R2e}^{+\bullet}$ ($-$) in CH_2Cl_2 (1.6×10^{-4} M).

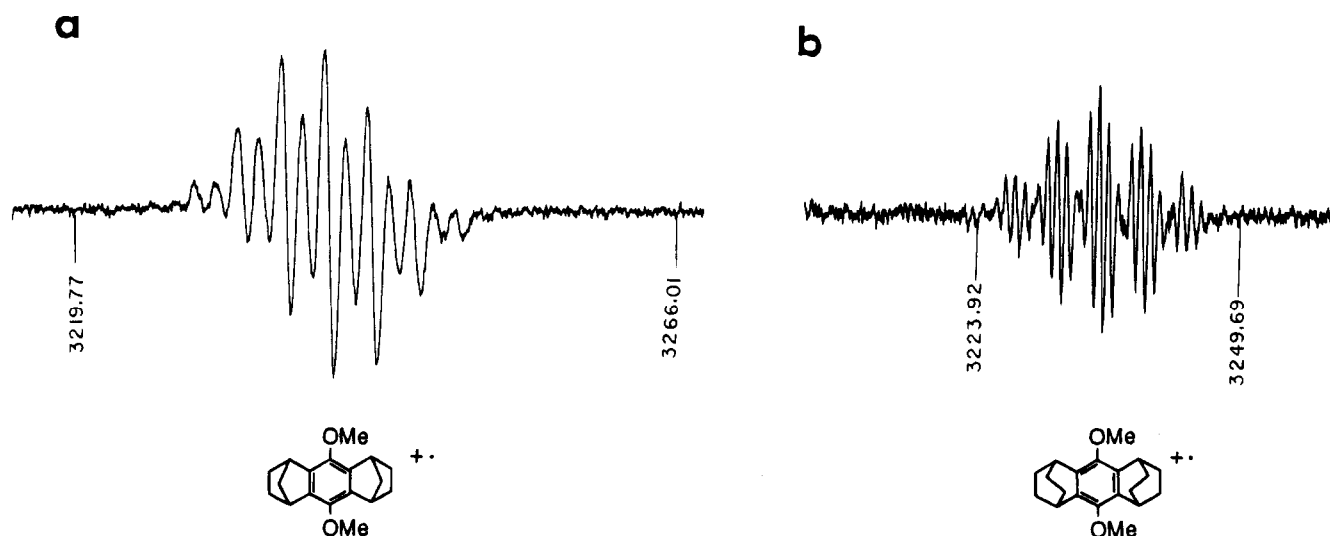


Figure 6. Experimental ESR spectrum of $\mathbf{R1a}^{+\bullet}$ obtained from the solution of the isolated crystalline salt $\mathbf{R1a}^{+\bullet}\text{SbCl}_6^-$ in dichloromethane at room temperature. ESR spectrum of the diethano analogue $\mathbf{R2a}^{+\bullet}$ under comparable conditions. The proton NMR field markers are in kHz.

The ESR spectra of the $\mathbf{R1a}^{+\bullet}$ salts (SbCl_6^- , BF_4^- , or PF_6^-) in dichloromethane solutions were measured at room temperature under an argon atmosphere. The spectrum of $\mathbf{R1a}^{+\bullet}$ was unchanged with different counterions, and it consisted of 15 (somewhat broadened) lines centered at $\langle g \rangle = 2.0023$, in comparison with the ESR spectrum of the diethano analogue $\mathbf{R2a}^{+\bullet}$ ³⁰ (see Figure 6).

Crystal Structure of the Radical Cation Salt of $\mathbf{R1a}$. Dark red crystals of $\mathbf{R1a}^{+\bullet}\text{SbCl}_6^-$ were grown by the liquid diffusion technique, employing dichloromethane and hexane (see the Experimental Section). Intensity data collection on a bright red multifaceted block of $\mathbf{R1a}^{+\bullet}\text{SbCl}_6^-$ was accomplished at -50 °C under conditions similar to those employed for the neutral analogue $\mathbf{R1a}$ (*vide supra*). The systematic absences revealed the

space group to be $P2_1/c$. Structure solution in this space group using the direct methods program SHELXTL furnished the positions of all non-hydrogen atoms in the asymmetric unit consisting of one-half cation and one-half anion situated about the inversion center. A perspective ORTEP view of the paramagnetic salt is shown in Figure 7a. The central ring of $\mathbf{R1a}^{+\bullet}$ is essentially planar with a maximum deviation of 0.0065 Å from the mean plane comprised of the atoms C1, C6, C8, C1', C6', and C8'. The bonds connected to C8 are longer than the usual value of 1.395 Å, and the angles about C8 deviate significantly from 120°. There is an in-plane skewing of the central ring as revealed from the nonorthogonality of the C1–C6–C1' angle. It is most noteworthy that both methoxy groups lie in the plane of the central ring (torsion angle involving the atoms C6–C8–O–C9 in $\mathbf{R1a}^{+\bullet}$ is 178.5°) unlike that observed in the neutral analogue $\mathbf{R1a}$ (torsion angle involving the atoms C6–C8–O–C9 in $\mathbf{R1a}$ is 99.1°). The selected bond lengths and bond angles are recorded in Table 4. The cell of $\mathbf{R1a}^{+\bullet}\text{SbCl}_6^-$ is composed of columns with alternating cations and anions as displayed in Figure 7b. Unfortu-

(29) For a related example of such a transient complexation, see: Sankararaman, S.; Haney, W. A.; Kochi, J. K. *J. Am. Chem. Soc.* **1987**, *109*, 5235.

(30) The complete analysis of the ESR spectra of the cation radicals derived from various tetrasubstituted hydroquinone alkyl ethers will be presented separately.

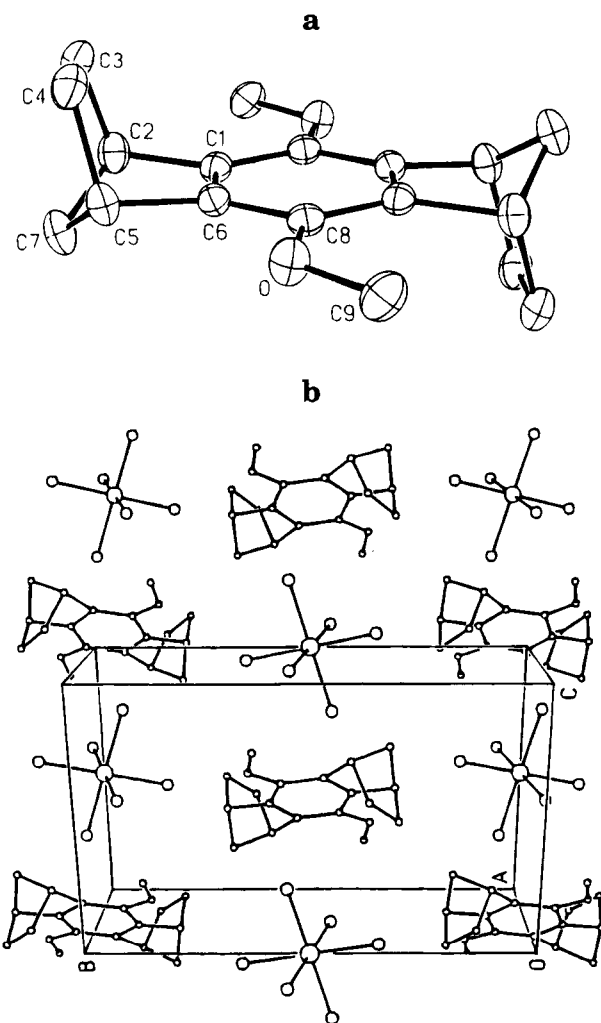


Figure 7. (a) ORTEP diagram of the radical cation salt ($\mathbf{R1a}^+\text{SbCl}_6^-$) showing the conformation of the methoxy groups to be coplanar with the aromatic plane. (b) Packing diagram of $\mathbf{R1a}^+\text{SbCl}_6^-$ in the unit cell, as viewed along the a axis.

Table 4. Selected Bond Distances (Å) and Angles (deg) for $\mathbf{R1a}^+\text{SbCl}_6^-$

distances		angles	
C8—O	1.320(4)	C8—O—C9	122.4(2)
C9—O	1.442(4)	C6—C8—O	113.6(2)
C6—C8	1.430(4)	C1—C6—C8	124.1(3)
C1—C6	1.378(4)	C5—C6—C8	127.5(3)
C1—C2	1.529(5)	C1—C6—C5	108.1(3)
C5—C6	1.506(4)	C2—C1—C6	105.6(2)
C5—C7	1.537(5)	C6—C5—C7	99.8(2)
C2—C7	1.536(4)	C4—C5—C6	104.6(2)
C4—C5	1.563(4)	C1—C2—C3	105.2(2)
C2—C3	1.551(4)	C1—C2—C7	100.5(3)
C3—C4	1.547(5)	C3—C2—C7	100.7(2)

nately, numerous attempts to grow single crystals of the homologous radical-cation salt of $\mathbf{R2a}^+$ suitable for X-ray crystallography have been uniformly unsuccessful.

Discussion

The bis-annulated tetrasubstituted hydroquinone ethers ($\mathbf{R1-R3}$) are strong electron donors as judged by their rather low (reversible) oxidation potentials in the range of $E_{1/2} = 1.1\text{--}1.3$ V *vs* SCE, as listed in Table 2. The chemical oxidation of the hydroquinone ethers $\mathbf{R1-R3}$ with either SbCl_5 or NO^+BF_4^- produces a series of brightly colored radical cation salts which are readily

isolated in crystalline form. It is especially noteworthy that the radical cation salts prepared from the $\mathbf{R1}$ and $\mathbf{R3}$ ethers are extremely robust, and they may be stored at room temperature for several months without decomposition (for example, a sample of $\mathbf{R1a}^+\text{SbCl}_6^-$ placed in a capped bottle under an atmosphere of ordinary air was periodically used for more than 1 year without color change or noticeable decomposition, as monitored by spectrophotometric and iodometric methods). Furthermore, solutions of $\mathbf{R1a}^+\text{SbCl}_6^-$ in anhydrous dichloromethane are remarkably stable for weeks if protected from moisture. By comparison, the crystalline radical-cation salts derived from the $\mathbf{R2}$ ethers showed slight color changes upon prolonged storage at room temperature and a decrease in radical cation titer of $\sim 5\text{--}10\%$, as revealed by iodometric analysis.

The usefulness of radical cations in a variety of electron transfer-mediated organic reactions prompted us to examine their redox properties. A prior knowledge of such properties of the radical-cation salts is essential in determining the feasibility of effecting electron transfer with other donors. As described in Table 2, the cation radicals $\mathbf{R1a}^+$, $\mathbf{R2a}^+$, and $\mathbf{R3a}^+$ exhibit striking differences insofar as their reduction potentials $E_{1/2}$ differ substantially among themselves and relative to that of the corresponding tetramethyl analogue $\mathbf{1a}^+$ (see Table 2). Indeed, the various methyl derivatives of hydroquinone ethers do not display a monotonic decrease in their oxidation potentials with increasing number of substituents. Instead, they exhibit the unpredictable trend described earlier.¹⁰ As such, the dramatic differences in the oxidation potentials of the annulated hydroquinone ethers $\mathbf{R1}$, $\mathbf{R2}$, and $\mathbf{R3}$ (involving as they do marginal structural alterations) now present an opportunity to analyze the interesting differences in $E_{1/2}$ in more detail. For example, the angle strain introduced into $\mathbf{R2}$ in going to $\mathbf{R3}$ and then to $\mathbf{R1}$ could be a factor in the observed variations of the oxidation potentials. Such a consideration, however, is ruled out by taking into account the observation that the simple tris-annulated analogues of $\mathbf{R1}$ and $\mathbf{R2}$ show a similar electrochemical behavior.³¹ Accordingly, let us now consider how the conformational changes of the alkoxy groups can play a crucial role in determining the donor strengths of substituted hydroquinone ethers and lead to an attendant stability of their radical-cation salts.

In order to quantitatively unravel the subtle structural changes of these hydroquinone methyl ethers, X-ray crystallographic analyses were performed on $\mathbf{R1a}$ and $\mathbf{R2a}$ since this donor pair shows a maximum difference of 200 mV in their electrochemical oxidation potentials. Interestingly, the crystallographic results reveal that the methoxy groups in both these hydroquinone ethers lie perpendicular to the aromatic plane (see Figure 1), and no distortion is apparent in the benzene nucleus (see Table 1 for bond lengths and bond angles). Significantly, the bridgehead hydrogens (Bredt's rule protected) in the case of $\mathbf{R2a}$ lie precisely in the plane of the aromatic ring, while the bridgehead hydrogens in $\mathbf{R1a}$ are moved away from the aromatic plane and the methoxy group, as illustrated in Chart 1.

(31) For example, the corresponding tris-annulated (methano and ethano) hydrocarbons³² are reversibly oxidized at a platinum electrode in dichloromethane solution at $E_{1/2} = 1.50$ and 1.54 V, respectively, *vs* SCE.

(32) (a) Gassman, P. G.; Gennick, I. *J. Am. Chem. Soc.* **1980**, *102*, 6863. (b) Komatsu, K.; Aonuma, S.; Jimbu, Y.; Tsuji, R.; Hirose, C.; Takeuchi, K. *J. Org. Chem.* **1991**, *56*, 195.

In order to further examine the conformational effects in solution, variable-temperature NMR analysis was carried out on the ethyl ether analogues of **R1a**, **R2a**, **R3a** and the acyclic derivative **1b**. The ethyl ether derivatives were specifically selected since any desymmetrization resulting from a conformational fixation can be easily recognized from the diastereotropic nature of the methylene protons. It is thus noteworthy that the methylene protons of **R2b** and diethoxydurene **1b** exhibit a normal quartet (due to the high facial symmetry in the molecules). On the other hand, the methylene protons of **R1b** and **R3b** display a symmetrical multiplet characteristic of an ABM₃ pattern (see Figure 2), which remains unchanged over a wide temperature range (−60 to 140 °C). The invariance of the methylene multiplet as a function of temperature in various tetrasubstituted hydroquinone ethers is strongly suggestive of a restricted rotation of the aromatic–alkoxy bond.³³ Such a restricted rotation of the Ar–O bond in tetrasubstituted hydroquinone ethers is consistent with the steric effect of the bridgehead hydrogens which acts to inhibit free rotation of the alkoxy groups (*vide supra*).

Crystallographic and NMR spectroscopic analyses show that the alkoxy groups in tetrasubstituted hydroquinone ethers lie perpendicular to the aromatic plane, and they reveal no other obvious differences in structures to account for the observed disparity in the oxidation potentials of **R1** to **R3**. In order to probe this anomaly further, let us consider the energetics of electron detachment from various hydroquinone ethers by photoelectron spectroscopy. The time resolution of less than 10^{−15} s for the vertical ionization energy (IP) to be measured by photoelectron spectroscopy represents the electron detachment from a (frozen) rotational state of the molecule³⁴ (note that vibrational effects are observed on the time scale of ~10^{−13} s). As such, the almost identical values of IP = 7.83 ± 0.01 eV in Table 3 indicate that there is essentially no change in the energy difference between the electronic state of the neutral donor (**R1a**, **R2a**, and **R3a**) and the cation radical (**R1a**^{•+}, **R2a**^{•+}, and **R3a**^{•+}, respectively). The corresponding acyclic tetramethyl derivative **1a** shows an ionization potential of 8.06 eV, in accord with the decreased electron-releasing effect of the methyl substituents compared to the bulkier alkyl groups in the series **R1**, **R2**, and **R3**. Contrastingly, the anodic electron detachment from neutral organic donors in solution is measured with a considerably longer time resolution of less than 10^{−6} s,³⁵ and thus, the value of *E*_{1/2} reflects the energetically favorable structural changes that occur in the resulting radical cations. As such, we conclude that the substantially larger value of *E*_{1/2} for **R2** relative to that of **R1** (see Table 3) points to a time dependent structural change in the cation-radical **R1**^{•+} or **R2**^{•+}.

The direct relationship between the vertical ionization potential and the adiabatic oxidation potential as two distinct measures of electron detachment is noteworthy. For example, Howell *et al.*¹² have demonstrated that a related series of alkyl-substituted benzene donors show

a linear correlation between the oxidation potentials (*E*_{1/2}) and the ionization potentials (IP) with a high correlation coefficient according to eq 6. The corresponding relation-

$$E_{\text{Ar}^{\bullet+}} = 0.71\text{IP} - 3.68 \quad (6)$$

ship between the oxidation potentials (*E*_{1/2}) and the gas-phase ionization potentials (IP) for various hydroquinone ethers shows considerable scatter (Figure 4). However, a close inspection of the data shows that the points for the unsubstituted, disubstituted, and diethano ether **R2a** are linearly related, but the points for the methano-bridged analogues **R1a** and **R3a** are clearly deviant. Since it appeared that the methano bridges are in some way related to the observed dramatic decrease in the oxidation potentials of **R1** and **R3**, the structure of the radical–cation salt derived from **R1a** was investigated by single crystal X-ray analysis. Indeed, the crystal structure of the radical cation salt **R1a**^{•+}SbCl₆[−] in Figure 7a shows that the methoxy groups lie in the plane of the (slightly skewed) aromatic ring. Since the methoxy groups in the corresponding neutral analogue are perpendicular to the aromatic plane (Figure 1a), a significant conformational change is associated with the transition from a neutral hydroquinone ether to the radical cation attendant upon electron transfer. Such a conformational reorganization seems to be facilitated by the (favorable) positions of the bridgehead hydrogens that lie slightly out of the aromatic plane and away from the methoxy group (see Chart 1). This conclusion is consistent with the observed “misfit” of **R1a** and **R3a** in the plot of IP vs *E*_{1/2} shown in Figure 4. Taking into account the correlation of *E*_{1/2} of the ethano-bridged analogue **R2a** with *E*_{1/2} of simple acyclic analogues in Figure 4, we believe that an analogous conformational switch does not occur as a result of electron detachment from **R2a**, especially since the bridgehead hydrogens in **R2a** lie in the plane of the aromatic ring to inhibit the methoxy groups from attaining the coplanar conformation. A validation of this analysis necessitates the crystal structure determination of **R2a**^{•+}. However, our inability to obtain single crystals of the more unstable **R2a**^{•+}SbCl₆[−] salt that are suitable for X-ray crystallography prevented such an examination at this time. Following these considerations, we also attribute the observed lower oxidation potential of **R3a** to its ability to undergo a similar structural organization during (or soon after) electron detachment. Thus, the methoxy groups in the radical cation salt of **R3a** should lie in the plane of the aromatic ring in a fashion which is *syn* to the methano bridge. Further, the relatively lower oxidation potential of the dimethano-bridged hydroquinone ether **R1a** as compared to that of the methano–ethano analogue **R3a** may be attributed to the accommodation of the methoxy groups in an *anti* fashion. Such a preference for the methoxy groups to lie in an *anti* conformation is also evident from resonance Raman study of 1,4-dimethoxybenzene radical cation in solution.³⁶

Additional evidence to favor a perpendicular conformation of the alkoxy groups in the ethano analogues **R2**^{•+} also comes from the following observations. The derivatives containing a tethered methoxy functionality, namely **R1e** and **R3e**, show an expected increase in their

(33) (a) Compare: Schaefer and Sebastian in ref 7a. (b) The quantitative effects of the ¹H NMR dynamics of methoxyarenes are beyond the scope of this study and will be reported later.

(34) Bock, H.; Ruppert, K.; Näther, C.; Havlas, Z.; Hermann, H. F.; Arad, C.; Gobel, I.; John, A.; Meuret, J.; Nick, S.; Rauschenbach, A.; Seitz, W.; Vaupel, T.; Soluki, B. *Angew. Chem., Int. Ed. Engl.* **1992**, *31*, 550.

(35) See: Bard, A. J.; Faulkner, L. R. *Electrochemical Methods*; Wiley: New York, 1980.

(36) (a) O'Neill, P.; Steenzen, S.; Schulte-Frohlinde, D. *J. Phys. Chem.* **1975**, *79*, 2773. (b) Ernstbrunner, E.; Girling, R. B.; Grossman, W. E. L.; Hester, R. E. *J. Chem. Soc., Perkin Trans. 2* **1978**, 177.

oxidation potentials (see Table 2) as compared to their methyl or ethyl ether derivatives, owing to the electron-withdrawing influence of alkoxy groups when situated in the β -position. On the other hand, no such change in the oxidation potential is observed in the case of **R2e**. One way this effect may be reconciled is by considering the stabilization of the radical cation by intramolecular solvation by the β -methoxy group as depicted earlier (see Chart 2). Such a stabilization of the radical cation would be feasible only when the conformation of the alkoxy group acquires a position perpendicular to the aromatic plane. If one assumes no major differences in going from **R1a** and **R3a** to **R1e** and **R3e**, respectively, the coplanar conformation of the alkoxy functionalities (*i.e.* CH₂CH₂-OMe) with the aromatic ring cannot be expected to stabilize the radical cation by intramolecular solvation. Indeed, the UV-vis absorption spectra of the radical-cation salts **R1e** and **R3e** show no change as compared to their corresponding methyl ether analogues, whereas **R2e** radical-cation salt exhibited significant changes in the shape of the spectral band as well as in the shift of the absorption maxima as shown in Figure 5c.

Summary and Conclusions

The graded series of bis-annulated tetrasubstituted *p*-hydroquinone methyl ethers **R1a–R3a** present an unique opportunity to examine the conformational effects of the methoxy group on aromatic donors. For example, the subtle structural difference between the methano-bridged **R1a** and the ethano-bridged **R2a** is reflected in the bridgehead hydrogens of **R1a** which are displaced away from the aromatic phase owing to the increased strain imposed by the methano bridge, as illustrated in Chart 1. As a result, the pair of methoxy groups can both occupy the favorable coplanar conformation with the aromatic plane (see Figure 2a) for maximum delocalization of the positive charge in the radical cation **R1a**^{•+}. Accordingly, we predict the significantly poorer donor properties of the diethano analogue **R2a** (by roughly 200 mV) to reside in the inability of the methoxy groups in the corresponding radical cation **R2a**^{•+} to enjoy an analogous conformation. Indeed, the enhanced stabilization of the methano-bridged **R1a**^{•+} is reflected in its unusual persistence in solution to dioxygen for much longer periods (weeks) than the ethano-bridged **R2a**^{•+}. In a more general context, the preferred coplanar conformation of the methoxy group in the radical cation now explains why 2,5-dimethyl-1,4-dimethoxybenzene (with two open *ortho* positions) is a significantly better electron donor than durohydroquinone methyl ether, despite the presence of two fewer electron-donating methyl groups.¹¹

Experimental Section

Preparation of 9,10-Dialkoxy-1,4:5,8-dimethano-1,2,3,4,5,6,7,8-octahydroanthracene (R1). Cyclopentadiene-*p*-benzoquinone Diels-Alder Adduct (**2**). To an ice-cold solution of *p*-benzoquinone (21.6 g, 0.2 mmol) in ethanol (200 mL) was added freshly prepared cyclopentadiene (26.4 g, 0.4 mol), and the mixture was stirred for 0.5 h. The colorless solid was filtered and washed with cold ethanol to furnish the bis-cyclopentadiene-quinone adduct **2** in almost quantitative yield (47 g). A solution of the adduct (24 g, 0.1 mol) in an ethyl acetate-ethanol (1:1) mixture (250 mL) containing 10% Pd on charcoal (200 mg) was hydrogenated in a Parr apparatus at 50 psi. When the uptake of hydrogen ceased (3 h), the catalyst was separated by filtration through a short pad of Celite, and the pad was washed with dichloromethane (200 mL). The

filtrate was evaporated *in vacuo* to furnish the tetrahydro diketone **3** as a colorless crystalline solid in quantitative yield (24 g).

Bromination of Adduct 3. Dodecahydro-1,4:5,8-dimethano-9,10-anthraquinone (**3**) (24.4 g, 100 mmol) was dissolved in chloroform (100 mL) at room temperature and a solution of Br₂ (16 g, 100 mmol) in chloroform (100 mL) added dropwise over 0.5 h under an argon atmosphere. The resulting suspension was stirred at room temperature for 3 h. Most of HBr produced in the reaction was blown off by bubbling argon through the reaction mixture. The resultant suspension was cooled in an ice-acetone bath, and the precipitate was filtered *in vacuo* and washed with cold chloroform to afford the hydroquinone **4** in 98% yield (24 g).

Alkylation of the Hydroquinone. The hydroquinone **4** (4.8 g, 20 mmol) was added under an argon atmosphere to a solution of sodium ethoxide (freshly prepared from sodium metal (1.38 g, 60 mmol) and ethanol at room temperature) in ethanol (50 mL). The mixture was stirred for 20 min, and iodomethane (7.1 g, 50 mmol) was then added all at once. The reaction mixture was refluxed for 4 h, cooled to 25 °C, diluted with water (250 mL), and extracted with dichloromethane (3 × 50 mL). The dichloromethane layer was successively washed with 10% aqueous NaOH solution, water, and brine and then dried over anhydrous magnesium sulfate. Removal of solvent *in vacuo* afforded the crude material which was filtered through a silica gel (100 g) column using dichloromethane as eluant. Recrystallization from a dichloromethane-ethanol mixture afforded pure **R1a** (5.2 g, 96%). The other dialkyl ethers (**R1**) were prepared by a similar procedure from the corresponding alkyl halides and **4**. The characteristic spectral data are given below.

9,10-Dimethoxy-1,4:5,8-dimethano-1,2,3,4,5,6,7,8-octahydroanthracene (R1a): mp 111–112 °C (CH₂Cl₂-EtOH); IR (KBr) 2983, 2969, 2960, 2951, 2921, 2869, 2863, 2823, 1483, 1307, 1201, 1108, 1049, 1019, 951 cm⁻¹; ¹H NMR (CDCl₃) δ 1.15 (sym m, 4H), 1.41 (br d, *J* = 8.4 Hz, 2H), 1.66 (dt, *J* = 8.4, 1.5 Hz, 2H), 1.85 (br d, *J* = 7.2 Hz, 4H), 3.53 (br s, 4H), 3.80 (s, 6H); ¹³C NMR (CDCl₃) δ 26.99, 40.56, 48.87, 61.20, 137.48, 143.47; GC-MS *m/z* 270 (M⁺), 270 calcd for C₁₈H₂₂O₂. Anal. Calcd for C₁₈H₂₂O₂: C, 79.96; H, 8.20. Found: C, 79.81; H, 8.21.

9,10-Diethoxy-1,4:5,8-dimethano-1,2,3,4,5,6,7,8-octahydroanthracene (R1b): mp 141–142 °C (CH₂Cl₂-EtOH); IR (KBr) 2984, 2966 (vs), 2936, 2867, 1485, 1465, 1381, 1309 (vs), 1270, 1200, 1112, 1049 (vs), 1030, 961, 916 cm⁻¹; ¹H NMR (CDCl₃) δ 1.14 (sym m, 4H), 1.34 (t, *J* = 7.2 Hz, 6H), 1.40 (sym d, 2H), 1.63 (sym d, 2H), 1.83 (sym d, 4H), 3.48 (br s, 4H), 3.98 (AB of ABM₃ system, $\Delta\nu_{AB}$ = 31.57 Hz, *J*_{AB} = 9.6 Hz, *J*_{AM} = 7.2 Hz, and *J*_{BM} = 7.2 Hz, 4H); ¹³C NMR (CDCl₃) δ 15.80, 26.94, 40.68, 48.91, 69.15, 137.91, 142.22; GC-MS *m/z* 298 (M⁺), 298 calcd for C₂₀H₂₆O₂.

9,10-Diisopropoxy-1,4:5,8-dimethano-1,2,3,4,5,6,7,8-octahydroanthracene (R1c): mp 162–163 °C (CH₂Cl₂-EtOH); IR (KBr) 2990, 2972 (vs), 2962, 2770, 1475, 1366, 1305 (vs), 1202, 1112 (vs), 1043, 977 (vs), 934 cm⁻¹; ¹H NMR (CDCl₃) δ 1.15 (m, 4H), 1.73 (m, 2H), 1.60 (m, 2H), 1.81 (m, 4H), 1.20 (d, *J* = 6.0 Hz, 6H), 1.36 (d, *J* = 6.0 Hz, 6H), 3.52 (s, 4H), 4.15 (sym m, 2H); ¹³C NMR (CDCl₃) δ 22.18, 23.19, 26.82, 40.88, 49.08, 74.90, 138.56, 141.01; GC-MS *m/z* 326 (M⁺), 326 calcd for C₂₂H₃₀O₂.

9,10-Bis(octyloxy)-1,4:5,8-dimethano-1,2,3,4,5,6,7,8-octahydroanthracene (R1d): mp 57–58 °C (EtOH); IR (KBr) 2988, 2976, 2965, 2956, 2925, 2919, 2869, 2853, 1466, 1378, 1312, 1269, 1202, 1124, 1066, 971 cm⁻¹; ¹H NMR (CDCl₃) δ 0.88 (t, *J* = 6.6 Hz, 6H), 1.15 (sym m, 4H), 1.25–1.88 (m, 36H), 3.49 (s, 4H), 3.91 (ABM₂ system, $\Delta\nu_{AB}$ = 19.2 Hz, *J*_{AB} = 9.37 Hz, *J*_{AM} = 6.59 Hz, and *J*_{BM} = 6.59 Hz, 4H); ¹³C NMR (CDCl₃) δ 14.09, 22.65, 26.13, 26.99, 29.30, 29.44, 30.36, 31.84, 40.72, 48.88, 73.88, 137.77, 142.54; GC-MS *m/z* 466 (M⁺), 466 calcd for C₃₂H₅₀O₂. Anal. Calcd for C₃₂H₅₀O₂: C, 82.35; H, 10.80. Found: C, 82.47; H, 10.90.

9,10-Bis(2-methoxyethoxy)-1,4:5,8-dimethano-1,2,3,4,5,6,7,8-octahydroanthracene (R1e): mp 86–87 °C; IR (KBr) 2988, 2968, 2945, 2923, 2867, 2814, 1481, 1554, 1313 (vs), 1207, 1129, 1065 (vs), 1030, 969, 918, 848 cm⁻¹; ¹H NMR

(CDCl₃) δ 1.12 (br d, J = 7.2 Hz, 4H), 1.38 (br d, J = 8.5 Hz, 2H), 1.61 (br d, J = 8.5 Hz, 2H), 3.42 (s, 6H), 3.50 (br s, 4H), 3.64 (sym m, 4H), 3.97 (sym m, 2H), 4.10 (sym m, 2H); ¹³C NMR (CDCl₃) δ 26.87, 40.57, 48.91, 59.02, 71.75, 72.63, 137.90, 142.40; GC-MS m/z 358 (M⁺), 358 calcd for C₂₂H₃₀O₄. Anal. Calcd for C₂₂H₃₀O₄: C, 73.71; H, 8.44. Found: C, 72.97; H, 8.42.

Preparation of 9,10-Dialkoxy-1,4:5,8-diethano-1,2,3,4,5,6,7,8-octahydroanthracene (R2). A solution of *p*-benzoquinone (10.8 g, 0.1 mol) in freshly distilled cyclohexadiene (40 g, 0.5 mol) was refluxed under an argon atmosphere for 12 h. Removal of excess cyclohexadiene afforded the bis adduct as a pale brown solid in quantitative yield (26.5 g), and it was used without further purification. A solution of the cyclohexadiene-benzoquinone adduct (13.2 g, 0.05 mol) in an ethanol-ethyl acetate mixture (200 mL) containing 10% Pd on charcoal (200 mg) was hydrogenated in a Parr apparatus at 80 psi for 12 h. The reaction mixture was filtered through a silica gel (100 g) column, and the column was washed with dichloromethane (200 mL). Evaporation of the filtrate afforded the pure tetrahydro derivative as a colorless crystalline solid (13.2 g, 97%). Bromination of perhydro-1,4:5,8-diethano-9,10-anthraquinone (10.9 g, 0.04 mol) with equimolar Br₂ (6.4 g, 0.04 mol) in chloroform (200 mL), according to the procedure described above, afforded the corresponding hydroquinone in essentially quantitative yield (10.8 g, 100%). Alkylation of the hydroquinone as described above furnished the corresponding ethers (R2) in excellent yields. The characteristic spectral data for various ethers are given below.

9,10-Dimethoxy-1,4:5,8-diethano-1,2,3,4,5,6,7,8-octahydroanthracene (R2a): mp 175–176 °C (ether-hexane); IR (KBr) 2943 (vs), 2859, 2822, 1473, 1357, 1332, 1309, 1233, 1129, 1104, 1047, 987, 815, 770, 633 cm⁻¹; ¹H NMR (CD₂Cl₂) δ 1.34 (br d, J = 7.2 Hz, 8H), 1.79 (br d, J = 1.72 Hz, 8H), 3.34 (br s, 4H), 3.68 (s, 6H); ¹³C NMR (CD₂Cl₂) δ 26.40, 27.34, 62.84, 134.36, 146.26; GC-MS m/z 298 (M⁺), 298 calcd for C₂₀H₂₆O₂. Anal. Calcd for C₂₀H₂₆O₂: C, 80.50; H, 8.78. Found: C, 80.78; H, 8.77.

9,10-Diethoxy-1,4:5,8-diethano-1,2,3,4,5,6,7,8-octahydroanthracene (R2b): mp 179–180 °C (EtOH); IR (KBr) 2970, 2944, 2925, 2907, 2891, 2863, 1463, 1389, 1364, 1332, 1309, 1233, 1131, 1100, 1049 (vs), 899, 817, 791, 633 cm⁻¹; ¹H NMR (CDCl₃) δ 1.32 (br d, 8H), 1.37 (t, J = 6.9 Hz, 6H), 1.72 (br d, 8H), 3.30 (br s, 4H), 3.79 (q, J = 6.9 Hz, 4H); ¹³C NMR (CDCl₃) δ 15.78, 26.01, 27.12, 70.74, 133.84, 144.58; GC-MS m/z 326 (M⁺), 326 calcd for C₂₂H₃₀O₂.

9,10-Bis(2-methoxyethoxy)-1,4:5,8-diethano-1,2,3,4,5,6,7,8-octahydroanthracene (R2e): mp 117–118 °C (ether-hexane); IR (KBr) 2979, 2941, 2907, 2880, 2862, 2818, 1465, 1456, 1331, 1307, 1278, 1229, 1198, 1127, 1102, 1061, 1034, 905, 852, 790 cm⁻¹; ¹H NMR (CDCl₃) δ 1.29 (br d, J = 7.2 Hz, 8H), 1.70 (br d, J = 7.2 Hz, 8H), 3.33 (br s, 4H), 3.66 (t, J = 5.1 Hz, 4H), 3.86 (t, J = 5.1 Hz); ¹³C NMR (CDCl₃) δ 25.90, 26.90, 59.01, 71.82, 73.42, 133.80, 144.63; GC-MS m/z 386 (M⁺), 386 calcd for C₂₄H₃₄O₄.

Preparation of 9,10-Dialkoxy-1,4-ethano-5,8-methano-1,2,3,4,5,6,7,8-octahydroanthracene (R3). To a solution of dihydronorbornobenzoquinone²⁰ (8) (10 g, 58 mmol) in toluene (50 mL) was added freshly distilled 1,3-cyclohexadiene (5.2 g, 65 mmol). The reaction mixture was heated at 50 °C for 5 h. Removal of the solvent *in vacuo* afforded the Diels-Alder adduct 9 in essentially quantitative yield (14.5 g, 57 mmol). The adduct 9 was added under an argon atmosphere to a freshly prepared solution of sodium ethoxide in ethanol (from 3.5 g of sodium metal in 200 mL of ethanol) at room temperature and stirred for 1 h. To the stirred solution was added all at once iodomethane (21 g, 148 mmol), and the reaction mixture was refluxed for 8 h. The reaction mixture was cooled to 25 °C, poured into water (500 mL), and then extracted with dichloromethane (3 × 100 mL). The combined organic layer was washed with NaOH, water, and brine and then dried over anhydrous magnesium sulfate. Removal of solvent furnished a crude material which was filtered through a silica gel (250 g) column and recrystallized from dichloromethane-hexane to afford pure 10a (14.4 g, 90%): mp 120–121 °C (CH₂Cl₂-hexane); IR (KBr) 2977, 2957, 2936, 2924, 2870, 2818, 1475,

1459, 1444, 1426, 1346, 1309 (vs), 1270, 1202, 1116, 1106, 1092, 1051, 1008, 987, 826, 729, 706 cm⁻¹; ¹H NMR (CDCl₃) δ 1.15–1.93 (m, 10H), 3.53 (br s, 2H), 3.78 (s, 6H), 4.27 (br s, 2H), 6.47 (quintet, J = 3.8 Hz, 2H); ¹³C NMR δ 25.50, 27.12, 33.62, 40.45, 49.18, 61.78, 134.65, 135.49, 136.70, 144.09; GC-MS m/z 282 (M⁺). In a Parr hydrogenation bottle was placed 2.84 g (10 mmol) of 10a dissolved in a mixture of ethanol and ethyl acetate (50 mL) containing 200 mg of 10% Pd on charcoal. The mixture was stirred at 80 psi of hydrogen at 25 °C for 3 h. Filtration through a short pad of silica gel (100 g) and evaporation of the solvent afforded the dihydro derivative R3a (2.82 g, ~100%) which was recrystallized from an ethanol-dichloromethane mixture. The derivatives R3b and R3e were prepared by a similar procedure, and the characteristic spectral data are given below.

9,10-Dimethoxy-1,4-ethano-5,8-methano-1,2,3,4,5,6,7,8-octahydroanthracene (R3a): mp 108–109 °C (CH₂Cl₂-EtOH); IR (KBr) 2987, 2972, 2951 (vs), 2937, 2867, 2819, 1475, 1461, 1446, 1331, 1309, 1295, 1268, 1207, 1110, 1053, 1039, 987, 950, 864, 819 cm⁻¹; ¹H NMR (CDCl₃) δ 1.20–1.95 (m, 14H), 3.31 (br s, 2H), 3.57 (br m, 2H), 3.74 (s, 6H); ¹³C NMR δ 25.93, 26.90, 27.18, 40.55, 49.01, 61.89, 134.28, 136.97, 144.61; GC-MS m/z 284 (M⁺), 284 calcd for C₁₉H₂₄O₂. Anal. Calcd for C₁₉H₂₄O₂: C, 80.23; H, 8.51. Found: C, 80.31; H, 8.69.

9,10-Diethoxy-1,4-ethano-5,8-methano-1,2,3,4,5,6,7,8-octahydroanthracene (R3b): mp 132–133 °C (ether-EtOH); IR (KBr) 2970, 2948, 2923, 2906, 2866, 1483, 1463, 1385, 1329, 1311, 1270, 1229, 1207, 1108, 1053, 965, 903 cm⁻¹; ¹H NMR δ 1.19–1.32 (m, 7H), 1.35 (t, J = 6.9 Hz, 6H), 1.44 (br d, J = 8.7 Hz, 1H), 1.69 (sym m, 4H), 1.88 (sym m, 2H), 3.31 (br s, 2H), 3.53 (br s, 2H), 3.90 (AB of ABM₃ system, $\Delta\nu_{AB}$ = 28.6 Hz, J_{AB} = 14.1 Hz, J_{AM} = 7.2 Hz, and J_{BM} = 7.2 Hz, 4H); ¹³C NMR (CDCl₃) δ 15.77, 25.92, 27.11, 40.68, 49.04, 69.83, 134.36, 137.92, 143.33; GC-MS m/z 312 (M⁺), 312 calcd for C₂₁H₂₈O₂.

9,10-Bis(2-methoxyethoxy)-1,4-ethano-5,8-methano-1,2,3,4,5,6,7,8-octahydroanthracene (R3e): 78–79 °C (ether-ethanol); IR (KBr) 2976, 2946, 2867, 2815, 1474, 1455, 1327, 1311, 1271, 1215, 1127, 1112, 1033, 906, 851 cm⁻¹; ¹H NMR δ 1.15–1.33 (m, 7H), 1.43 (d, J = 8.4 Hz, 1H), 1.67 (sym m, 4H), 1.87 (sym m, 2H), 3.22 (br s, 2H), 3.43 (s, 6H), 3.54 (br s, 2H), 3.66 (sym m, 4H), 3.96 (AB of ABM₂ system, $\Delta\nu_{AB}$ = 22.1 Hz, J_{AB} = 10.2 Hz, J_{AM} = 5.1 Hz, and J_{BM} = 4.5 Hz, 4H); ¹³C NMR (CDCl₃) δ 25.87, 26.96, 27.08, 40.60, 49.09, 59.05, 71.84, 73.28, 137.38, 137.21, 143.50; GC-MS m/z 372 (M⁺), 372 calcd for C₂₃H₃₂O₂.

Preparation of Diethoxydurene (1b). Durohydroquinone (1.64 g, 10 mmol) was converted to the diethoxydurene with sodium ethoxide and ethyl iodide in ethanol according to the procedure described above (2.0 g, 90%): mp 93–95 °C (EtOH); IR (KBr) 2998, 2977, 2923, 2880, 1542, 1467, 1385, 1369, 1252, 1113, 1081, 1041, 1010, 909, 853, 698 cm⁻¹; ¹H NMR (CDCl₃) δ 1.41 (t, J = 6.9 Hz, 6H), 2.17 (s, 12H), 3.73 (q, J = 6.9 Hz, 4H); ¹³C NMR (CDCl₃) δ 12.79, 15.54, 68.23, 127.54, 151.60; GC-MS m/z 222 (M⁺), 222 calcd for C₁₄H₂₂O₂.

Materials. Dichloromethane (Mallinckrodt analytical reagent) was repeatedly stirred with fresh aliquots of concentrated sulfuric acid (~20% by volume) until the acid layer remained clear. After separation, it was washed successively with water, aqueous sodium bicarbonate, water, and aqueous sodium chloride and dried over anhydrous calcium chloride. The dichloromethane was distilled twice from P₂O₅ under an argon atmosphere and stored in a Schlenk tube equipped with a Teflon valve fitted with Viton O-rings. Acetonitrile (Fischer) was stirred with KMnO₄ for 24 h, and the mixture was refluxed until the liquid was colorless. The MnO₂ was removed by filtration. The acetonitrile was distilled from P₂O₅ under an argon atmosphere and then refluxed over CaH₂ for 6 h. After distillation from the CaH₂, the solvent was stored in a Schlenk flask under an argon atmosphere. Nitrosodium tetrafluoroborate (Strem) was stored in a Vacuum Atmospheres HE-493 drybox kept free of oxygen. Tetra-*n*-butylammonium hexafluorophosphate, antimony pentachloride, tetra-*n*-butylammonium iodide, 1,4-dimethoxybenzene, *p*-benzoquinone, and 1,3-cyclohexadiene were commercially available (Aldrich) and were

used as received. 1,4-Dimethoxydurene (**1**) and 2,5-dimethyl-1,4-dimethoxybenzene were prepared from literature procedures.¹⁰

Instrumentation. The UV-vis absorption and IR spectra were recorded on a Hewlett-Packard 8450A diode-array spectrometer and a Nicolet 10DX FT spectrometer, respectively. Gas-phase IR spectra were recorded with a 5 cm path length cell. The ¹H and ¹³C NMR spectra were recorded on a General Electric QE-300 spectrometer, and chemical shifts are reported in ppm units downfield from tetramethylsilane. Gas chromatography was performed on a Hewlett-Packard 5890A series FID gas chromatograph fitted with a 3392 integrator. GC-MS analyses were carried out on a Hewlett-Packard 5890 chromatograph interfaced to a HP 5970 mass spectrometer (EI, 70 eV). The photoelectron spectra of the hydroquinone methyl ethers **R1a**, **R2a**, and **R3a** were recorded using He I (21.2 eV) radiation at 94, 110, and 95 °C, respectively.³⁷

Cyclic Voltammetry of *p*-Dialkoxyarenes. Cyclic voltammetry (CV) was performed on a BAS 100B Electrochemical Analyzer. The CV cell was of an airtight design with high-vacuum Teflon valves and Viton O-ring seals to allow an inert atmosphere to be maintained without contamination by grease. The working electrode consisted of an adjustable platinum disk embedded in a glass seal to allow for periodic polishing (with a fine emery cloth) without the surface area (~1 mm²) being changed significantly. The SCE reference electrode and its salt bridge were separated from the catholyte by a sintered glass frit. The counterelectrode consisted of a platinum gauze that was separated from the working electrode by ~3 mm. The CV measurements were carried out in a solution of 0.2 M supporting electrolyte (tetra-*n*-butylammonium hexafluorophosphate) and 5 × 10⁻³ M dialkoxybenzene in dry dichloromethane under an argon atmosphere. All the cyclic voltammograms were recorded at the sweep rate of 100 mV s⁻¹ and were IR-compensated. The potentials were referenced to SCE which was calibrated with added ferrocene (5 × 10⁻³ M). The oxidation potential values were calculated by taking the average of the anodic and cathodic peak potentials, and the E_{1/2} values are listed in Table 2.

Preparative Scale Electrooxidation of Hydroquinone Ethers. The electrooxidations were carried out with a PAR Model 173 potentiostat/galvanostat equipped with PAR Model 179 digital coulometer which provided a feedback compensation for ohmic drop between the working and reference electrodes. The voltage-follower amplifier (PAR Model 178) was mounted externally to the potentiostat with a minimum length of high-impedance connection to the reference electrode. The electrochemical cell was of airtight design. The counterelectrode was constructed of a double coil of nichrome wire with a large surface area. The working electrode consisted of a platinum wire cage wrapped with a platinum gauze with a total surface area of ~1.1 cm². The electrooxidations were carried out at constant potential.

General Procedures for the Preparation of Radical-Cation Salts. Tetrafluoroborate Salts. A 50 mL flask fitted with a quartz cuvette and a Schlenk adaptor was charged with NO⁺BF₄⁻ (118 mg, 1 mmol), and a solution of **R1a** (270 mg, 1 mmol) in anhydrous dichloromethane was added under an argon atmosphere. The nitric oxide (NO) produced (UV-vis spectral analysis of the gas revealed the characteristic absorbances of NO at λ_{max} = 204, 214, and 226 nm²¹) was entrained by bubbling argon through the solution. The red-orange suspension was stirred for 30 min to yield a dark red solution of **R1a**^{•+} (λ_{max} (nm) = 518, 486 (sh); see Figure 2). The resultant red solution was cooled to -78 °C in a dry ice-acetone bath, and anhydrous diethyl ether was added. The red precipitate was filtered under an argon atmosphere and washed with diethyl ether to afford essentially

pure **R1a**^{•+}BF₄⁻ (by iodometric titration) in excellent yield (342 mg, 96%) using the same procedure. The ethers (**R1a-e**, **R2a**, and **R3a**) were also converted to the corresponding radical-cation salts using the same procedure.

Hexachloroantimonate Salts. The dimethyl ether **R1a** (5.4 g, 20 mmol) was dissolved in anhydrous dichloromethane (40 mL) under an argon atmosphere in a 200 mL flask equipped with a Schlenk adaptor. The flask was cooled in a dry ice-acetone bath (approximately -78 °C), and neat SbCl₅ (12.0 g, 40 mmol) was slowly added under a reverse flow of argon. The solution immediately turned deep orange-red, and a large amount of crystalline material precipitated. The resultant mixture was warmed to 0 °C, and anhydrous diethyl ether (100 mL) was added to precipitate the dissolved salt. The orange-red precipitate was filtered under an argon atmosphere and washed thoroughly with anhydrous ether. The crystalline **R1a**^{•+}SbCl₆⁻ salt was dried at room temperature (25 °C) *in vacuo* to afford fine, orange-red, needle-shaped crystals in essentially quantitative yield (12 g, 99%). Anal. Calcd for C₁₈H₂₂O₂SbCl₆: C, 35.74; H, 3.67; Cl, 35.17. Found: C, 35.72; H, 3.61; Cl, 33.59.

Solutions of Hexafluorophosphate Salts. The hydroquinone ether **R1a** (27 mg, 0.1 mmol) was dissolved in dichloromethane (30 mL) containing 0.1 M electrolyte (TBAPH). This mixture was placed in the center compartment of the electrochemical cell. The reference electrode and counterelectrode compartments were charged with the dichloromethane containing the 0.1 M electrolyte. The mixture was electrolyzed at a constant potential of 1.15 V for 15 min. The current flow recorded with the aid of a digitized coulometer was 6.5 C. The current flow was stopped at the end of this period owing to the mechanical clogging of the frits. The dark red solution of **R1a**^{•+}PF₆⁻ thus obtained was analyzed by UV-vis spectroscopy and was found to be identical with the BF₄⁻ and SbCl₆⁻ salts.

Determination of the Purity of Radical-Cation Salts by Iodometry. General Procedure. Solutions of the various radical-cation salts (0.2 mmol, 0.01 M) and TBAI (1 mmol, 0.1 M) in dichloromethane were mixed under an argon atmosphere at 25 °C to afford dark brown solutions. The mixture was stirred for 5 min and titrated (with rapid stirring) by the slow addition of a standard aqueous sodium thiosulfate solution (0.005 M).

X-ray Crystallography of Hydroquinone Ethers and Their Radical-Cation Salts. The intensity data for all compounds were collected with the aid of a Nicolet R3m/V automatic diffractometer under a stream of nitrogen at approximately -50 °C. The radiation used was Mo Kα, monochromatized by a highly ordered graphite crystal. In all the cases, 25 standard reflections were used to refine the cell parameters. The structures were solved by the program SHELXTL PLUS on the basis of direct methods and refined using a full-matrix least-squares method as follows.

9,10-Dimethoxy-1,4:5,8-dimethano-1,2,3,4,5,6,7,8-octahydroanthracene (R1a). The crystals of **R1a** were grown by slow evaporation of the solution in a diethyl ether-hexane mixture at room temperature. A colorless flat column with the dimensions 0.75 × 0.45 × 0.25 mm was mounted in a random orientation on a glass fiber. The crystal system was determined to be monoclinic with the space group P2₁/c; a = 7.976(1) Å, b = 15.290(3) Å, c = 5.841(1) Å, β = 92.53(1)°, V = 712 Å³, and Z = 2. Data were collected employing the θ-2θ scan technique in the range 4° < 2θ < 48°. Two standard reflections monitored after every 2 h of data collection showed no significant variations. The total number of reflections was 1269, of which 984 reflections were with I > 3σ(I₀). The structure solution in a routine manner revealed the positions corresponding to all non-hydrogen atoms in the asymmetric unit with one-half molecule situated about the inversion center. The subsequent usual sequence of isotropic and nonisotropic refinements was followed. All the hydrogens were fixed at calculated positions with isotropic temperature factors and were subsequently constrained to riding motion: no. of variables 93, R = 0.038 and R_w = 0.036.

9,10-Dimethoxy-1,4:5,8-diethano-1,2,3,4,5,6,7,8-octahydroanthracene (R2a). Slow evaporation of the diethyl

(37) See: Li, X.; Bancroft, G. M.; Puddephatt, R. J.; Liu, Z. F.; Hu, Y. F.; Tan, K.H. *J. Am. Chem. Soc.* **1994**, *116*, 9543.

(38) The author has deposited atomic coordinates for **R1a**, **R2a**, and **R1a**^{•+}SbCl₆⁻ with the Cambridge Crystallographic Data Centre. The coordinates can be obtained, on request, from the Director, Cambridge Crystallographic Data Centre, 12 Union Road, Cambridge, CB2 1EZ, U.K.

ether-hexane solution of **R2a** at room temperature yielded colorless plates. A suitable crystal with the dimensions 0.70 × 0.50 × 0.35 mm was cut from the end of a large thick column and mounted in a random orientation on a glass fiber. The crystal system was found to be triclinic with the space group $P\bar{1}$; $a = 9.321(2)$ Å, $b = 9.782(2)$ Å, $c = 10.124(3)$ Å, $\alpha = 72.47(2)^\circ$, $\beta = 66.14(2)^\circ$, $\gamma = 80.20(2)^\circ$, $V = 804$ Å³, and $Z = 2$. The data were collected in the range $4^\circ < 2\theta < 50^\circ$. Two standard reflections monitored every 2 h during data collection showed no significant variations. The total number of reflections measured was 2823, of which 2477 reflections were with $I > 3\sigma(I_0)$. The structure was solved using the direct methods program (SHELXTL-PLUS), which revealed the positions of all non-hydrogen atoms in the asymmetric unit consisting of two independent half-molecules situated about the inversion centers. The usual sequence of isotropic and anisotropic refinement was followed, after which all the hydrogen atoms were fixed in the ideal calculated positions: no. of variables 201, $R = 0.036$ and $R_w = 0.036$.

9,10-Dimethoxy-1,4:5,8-dimethano-1,2,3,4,5,6,7,8-octahydroanthracene Radical Cation (R1a⁺SbCl₆⁻). Bright red crystals were grown by using the vapor diffusion of hexane into a solution of **R1a⁺SbCl₆⁻** in anhydrous dichloromethane at room temperature. A multifaceted crystal with dimensions 0.24 × 0.26 × 0.33 mm was mounted on the tip of a glass fiber. The crystal was found to be monoclinic with the space group

$P2_1/c$; $a = 8.507(1)$ Å, $b = 14.448(2)$ Å, $c = 9.967(1)$ Å, $\beta = 112.32(1)^\circ$, $V = 1133$ Å³, and $Z = 2$. The intensities were measured using the θ - 2θ mode, and two standard reflections were regularly monitored after every 2 h of data collection. A total of 2166 reflections were collected, of which 1699 were found to satisfy the condition $I > 3\sigma(I_0)$. The structure solution in an analogous manner using the direct methods program furnished the positions of all the non-hydrogen atoms in the asymmetric unit consisting of one-half anion and one-half cation, both situated about the inversion centers. The isotropic and anisotropic refinement of the non-hydrogen atoms was performed using the full-matrix least-squares method, and the positions corresponding to hydrogens were fixed at calculated positions. At the end of the refinement, the final $R = 0.018$ and $R_w = 0.019$ for 126 variables.

Acknowledgment. We thank G. M. Bancroft and Y.-F. Hu (University of Western Ontario, Canada) for kindly measuring the photoelectron spectra, T. M. Bockman for recording the ESR spectra, J. D. Korp for crystallographic assistance, and the National Science Foundation, the R. A. Welch Foundation, and the Texas Advanced Research Project for financial assistance.

JO950401A